DOI 10.1007/s10946-023-10137-7
*Journal of Russian Laser Research, Volume 44, Number 3, May, 2023*

# STUDY OF TRANSIENT THERMAL EFFECTS IN A Nd : YAG LASER UNDER QUASI-CONTINUOUS LASER-DIODE END PUMPING

**Peijin Shang, Lu Bai, and Shiyu Wang***

*School of Optoelectronic Engineering, XiDian University*
*Xi'an Shaanxi 710071, China*

*Corresponding author e-mail: stone_whisper @ 163.com

**Abstract**

We develop a quasi-steady-state thermal model to analyze transient thermal effects in a Nd : YAG laser rod under quasi-continuous laser-diode (LD) end pumping. Included is a quasi-adiabatic model for pump durations and a quasi-steady-state heat dissipation model for pump-free durations. We give an approximate expression of the transient temperature-difference distribution function of the crystal under quasi-continuous pumping. The method for calculating the transient thermal focal length is also presented. On this basis, the temperature distribution variation in the crystal with time and the variation range of the transient thermal focal length are quantitatively analyzed. For 50 W, 200 μs pulse-width, and 50 Hz pumping, the temperature at the center of the Nd:YAG rod has a range of 304.52 – 306.28 K, and the thermal focal length varied over 1612.8 – 310.43 mm. Both have saw-tooth periodic distributions. This study provides a theoretical reference for the design of laser-diode-pumped thermal $Q$-switched Nd : YAG lasers.

**Keywords:** transient thermal effect, quasi-continuous LD end-pump, quasi-steady-state thermal model, transient thermal focal length, Nd : YAG rod.

## 1. Introduction

Laser-diode (LD)-pumped solid-state lasers have advantages such as small volumes, light weights, high efficiencies, long lives, and compact structures. Therefore, they are widely used in scientific research, industry, defense, and military applications [1–4]. With the development of semiconductor lasers, the output modes of LD-pumped solid-state lasers are mainly pulsed and continuous. Relative to continuous modes, pulsed modes have higher optical–optical conversion efficiencies and output energies [5].

When the thermal relaxation time is close to the pump period, thermal effects in pulsed LD end-pumped solid-state lasers are more complex. Each pump period can be divided into pump and pump-free durations. During the pump duration, the crystal temperature increases with continuous injection of high-energy pump light. During pump-free duration, the temperature decreases with the continuous operation of the cooling system. Therefore, the temperature field in the crystal fluctuates periodically, forming transient thermal lens effects, which affect the output characteristics of the laser pulse [6, 7].

Steady-state thermal effects in quasi-continuous end-pumped crystals are usually studied via such methods as the finite-element methods (FEMs) and finite-difference methods (FDMs) [8]. In 2009, Wang et al. [9] approximated a pulsed end-pumped Nd:YAG with a quasi-three-level system, and used variable separation methods to numerically simulate the radial temperature rise in the crystal. In 2010, Tian et

Manuscript submitted by the authors in English on March 23, 2023.

al. [10] established a three-dimensional steady-state heat conduction equation and used FDMs to simulate the temperature distribution in a Tm:YAP crystal. In 2011, Yao et al. [11] established a two-dimensional steady-state heat conduction equation in a cylindrical coordinate system and used FDMs to simulate radial and axial temperature distributions in Tm : YLF and Tm : YAP crystals.

With the above numerical analysis methods, two-dimensional and three-dimensional steady-state heat conduction equations based on spatial domains can be realized. However, during the process of solving the radial transient-temperature distribution in the crystal, large uncertainties are generated during iterations. Hence, results for transient thermal effects in the crystal will be significantly affected. At the same time, in the analysis of the transient heat conduction equation, the analytical solution becomes more complex. Moreover, the solution for various thermal boundary conditions are different; thus, the calculations are also difficult [12, 13].

Here, we analyze the temperature variation in a quasi-continuous LD end-pumped Nd : YAG crystal. Quasi-adiabatic and quasi-steady-state heat dissipation models are developed for pump and pump-free durations, respectively. Based on the generation mechanism of the thermal effects, we obtain the variation in the temperature-difference distribution function in the crystal during heat accumulation and dissipation. Under quasi-continuous periodic end-face pumping, the variation in the transient thermal focal length for a Nd : YAG rod is quantitatively analyzed.

The thermal analysis model can yield the change process for the crystal temperature field. It can also provide the variation in thermal focal length, when the system reaches the thermal equilibrium. In addition, for the case of a specific heat source distribution, the steady-state heat dissipation at any power can be quickly obtained via the thermal analysis model. Therefore, this model provides a theoretical basis for all solid-state lasers to produce high-power and narrow-pulse-width outputs and thus improve laser performance. Finally, it also provides a certain reference value for accurately understanding transient thermal effects in laser crystals, and to utilize them [14] when designing a thermally stable cavity.

## 2. Establishment of a Quasi-Steady-State Thermal Model under Quasi-Continuous LD Periodic Pumping

For quasi-continuous pump durations much shorter than pump-free durations (difference of two to four orders of magnitude), heat transfer processes in the crystal are ignored. After the pump duration, the crystal enters pump-free duration for heat dissipation. The temperature-difference distribution in the crystal during the pump-free duration is determined by the two factors of average pump power injected during the pump duration and the heat-dissipation boundary conditions (such as constant temperature or unbounded conditions). Therefore, for quasi-continuous LD periodic pumping, the quasi-adiabatic and quasi-steady-state heat dissipation models were respectively established to approximately describe temperature-change processes in the crystal during pump and pump-free durations.

### 2.1. Quasi-Adiabatic Model

As noted above, for short pump durations, heat transfer in the crystal is ignored. Therefore, for a crystal composed of infinitely many micro-elements, only the conduction characteristics of the beam are considered, and the conduction characteristics of the heat are ignored. In Fig. 1, we present the quasi-adiabatic model.

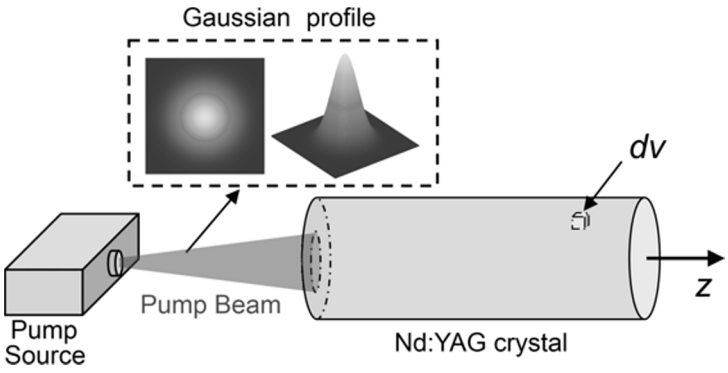


**Fig. 1.** Quasi-adiabatic model.

According to the first law of thermodynamics, the temperature increase in the crystal caused by the pump light can be approximately described by the temperature-difference distribution function $\Delta T_h$,

$$\Delta T_h = \frac{\rho_h V t}{cm}, \tag{1}$$

where $c$ and $m$ are the specific heat capacity and mass of the crystal, respectively. The numerator represents the pump energy absorbed by the crystal, and $\rho_h$ and $V$ are the thermal power density distributions injected into the crystal and its volume, respectively.

For an LD end-pumped Nd : YAG rod, the pump light output via optical fiber coupling can be described as follows [15]:

$$\rho_h = \frac{\alpha\eta 2P_{\text{in}}}{\pi\omega_p^2} \exp\left(-\frac{2r^2}{\omega_p^2}\right), \tag{2}$$

where $\eta$ is the heat transfer efficiency, $P_{\text{in}}$ is the pump power, $\alpha$ is the absorption coefficient, and $\omega_p$ is the pump light radius. Therefore, the transient temperature-field distribution in the crystal during the pump duration could be obtained via the quasi-adiabatic model.

## 2.2. Quasi-Steady-State Heat Dissipation Model

Analogously to the quasi-adiabatic model, a quasi-steady-state heat dissipation model is developed. According to the specific heat dissipation boundary conditions, the model assumes that the accumulated heat in the crystal during the pump duration forms a stable temperature-difference distribution during the pump-free duration for a certain average thermal power. The temperature and temperature-difference distribution at any point in the crystal are proportional to the power of the heat source. When the heat source stops, the temperature in the medium decreases synchronously in a specific proportion until it reaches the external temperature (i.e., thermal equilibrium). On this basis, the temperature-difference variation in the crystal during the pump-free duration can be obtained by transforming the transient heat conduction equation [16] to the following one:

$$\rho c \frac{\partial \Delta T_d}{\partial t} = \lambda \nabla^2 (\Delta T_d), \tag{3}$$

where $\rho$ and $c$ are the density and specific heat capacity of the Nd : YAG crystal, respectively, $\lambda$ denotes the thermal conductivity of the crystal, and $\Delta T_d$ is the temperature difference distribution function of the crystal during the pump-free duration. In view of the separation of variables method, $\Delta T_d$ is separated into the product of the time-variation function $M(t)$ and the temperature-difference distribution function $\phi_d$, it reads

$$\Delta T_d = \phi_d \cdot M(t). \tag{4}$$

One can obtain $M(t)$ using the temperature-field distribution at the beginning of the pump-free duration to properly select the coefficient of $\phi_d$,

$$M(t) = M_0\, e^{-(\beta\lambda/\rho c)t}, \tag{5}$$

where $M_0$ is the time varying coefficient, $\beta$ is a positive constant independent of space and time (it is determined by the boundary conditions), $\phi_d$ does not depend on time (it is only affected by the heat-dissipation boundary conditions and the spatial distribution function of the heat source during the pump duration).

For an LD end-pumped Nd : YAG rod, under constant-temperature boundary conditions, it is heated along the axial direction during the pump duration. The heat flow direction in the rod is approximately radial. Thus, the expression of heat flux $\vec{J}_h$ in rod can be obtained by Fourier's law [17],

$$\vec{J}_h(r) = -\lambda \frac{d\phi_d}{dr} \vec{e}_r. \tag{6}$$

For a cylinder with a center axis and radius $r$ as the unit length, we obtain the relationship between $\phi_d$ and $\rho_h$, using the Gauss theorem of integral transformation, and arrive at

$$-\lambda \int_0^r \frac{d\phi_d}{dr} \cdot 2\pi \, dr = \int_0^r \rho_h \cdot 2\pi r \, dr. \tag{7}$$

Then we obtain the final $\phi_d$, using the constant-temperature boundary condition; it reads

$$\phi_d(r) = \frac{\eta \alpha P_{in}}{2\pi\lambda} \left[ e^{-2r^2/\omega_p^2} - e^{-2r_0^2/\omega_p^2} \right]. \tag{8}$$

The continuity of heat transfer between the pump and pump-free durations can be described as follows:

$$-\frac{\partial \varepsilon_d}{\partial t}\bigg|_{t=0} = p_h, \tag{9}$$

where $\varepsilon_d$ is the residual thermal energy in the crystal during the pump-free duration, $p_h$ is the total thermal power stored in the crystal during the pump duration, and $\beta$ can be approximately obtained as

$$\beta = \frac{4\left[1 - \exp\left(-2\, r_0^2/\omega_p^2\right)\right]}{\left\{\left[-\omega_p^2\left(e^{-2\, r_0^2/\omega_p^2} - 1\right)\right] - \left[2\, r_0^2 \exp\left(-2\, \frac{r_0^2}{\omega_p^2}\right)\right]\right\}}. \tag{10}$$

Therefore, the transient temperature-field distribution in the crystal during the pump-free duration under the quasi-steady-state heat dissipation model is obtained.

## 3. Analysis of the Transient Temperature-Field Variation in a Nd : YAG Rod

In the quasi-steady-state thermal model, we assume that the pump light distribution is a circularly symmetric Gaussian. The pump power is 50 W, with a 200-μs pulse width and a 10-Hz repetition frequency. The length of Nd : YAG rod is 10 mm, and its diameter is 4 mm. During the first period, the transient temperature-difference distribution of the Nd : YAG rod is shown in Fig. 2.

The temperature decreases exponentially from the center point along the radial direction during the pump duration. The temperature-field distribution corresponds to the injected circularly symmetric Gaussian light distribution. With the injection of pump light, the temperature increases linearly with

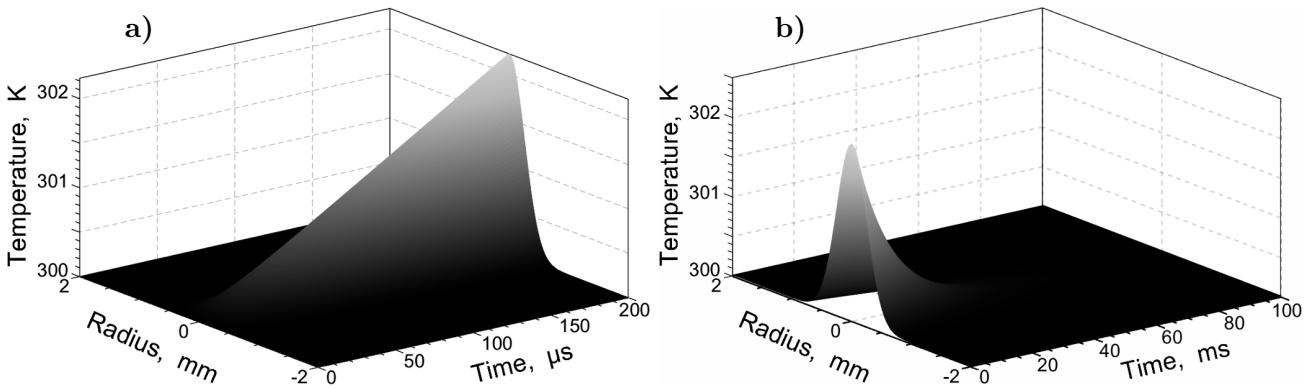


**Fig. 2.** Variation of temperature distribution during the pump duration (a) and during the pump-free duration (b).

time from 300 K. At the end of the pump duration, the center temperature of the crystal is 302.23 K. The temperature at the 0.6 mm radius (0.5 mm pump light radius) is approximately at the ambient temperature. The temperature of any point in the crystal is proportional to the pump power and pulse width.

The pump-free duration started at the end of the pump duration, and the temperature field decreases from the center to the radial direction. With heat conduction, the temperature decreases exponentially with time. When the pump-free duration is 40 ms, it is approximately reduced to the ambient temperature. The side of the crystal remains at a constant temperature because of the boundary conditions. In this process, the temperature at any point in the crystal is proportional to the pump power, pump time, and pump period. This is consistent with our quasi-steady-state heat dissipation model. To verify the continuity of the temperature distribution, that of the first and tenth pump periods are shown in Fig. 3.

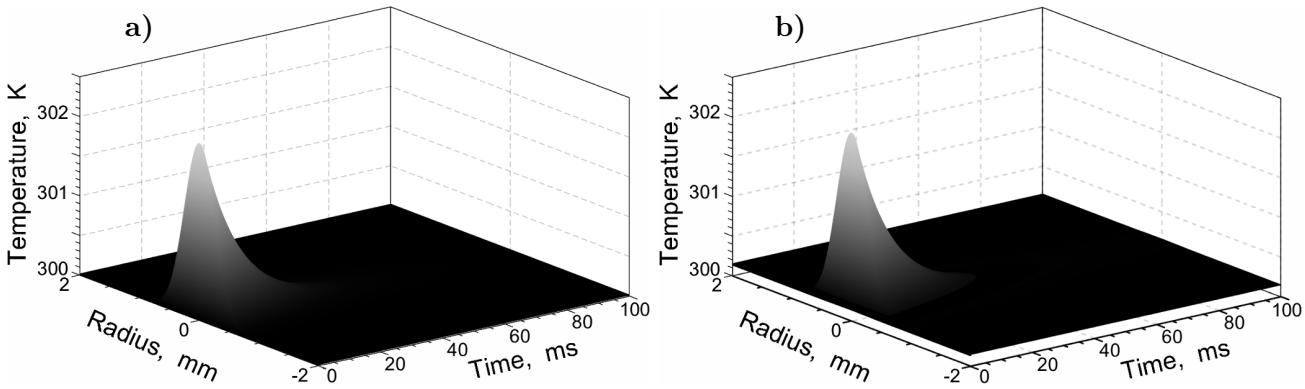


**Fig. 3.** Variation of temperature distribution with time at 10 Hz at the first pump period (a) and at the tenth pump period (b).

In Fig. 3, the pump duration is short, and the temperature increases rapidly at a low repetition rate. The radial temperature field in the crystal is approximately uniform for a 50-ms pump duration. Relative to the first period in Fig. 3 a, the temperature field in the tenth pump period (Fig. 3 b) has a small 0.15 K temperature increase, but the overall trend is the same.

To verify the continuity of the temperature field described by the quasi-steady-state heat dissipation model, we increase the repetition frequency to 50 Hz; see Fig. 4.

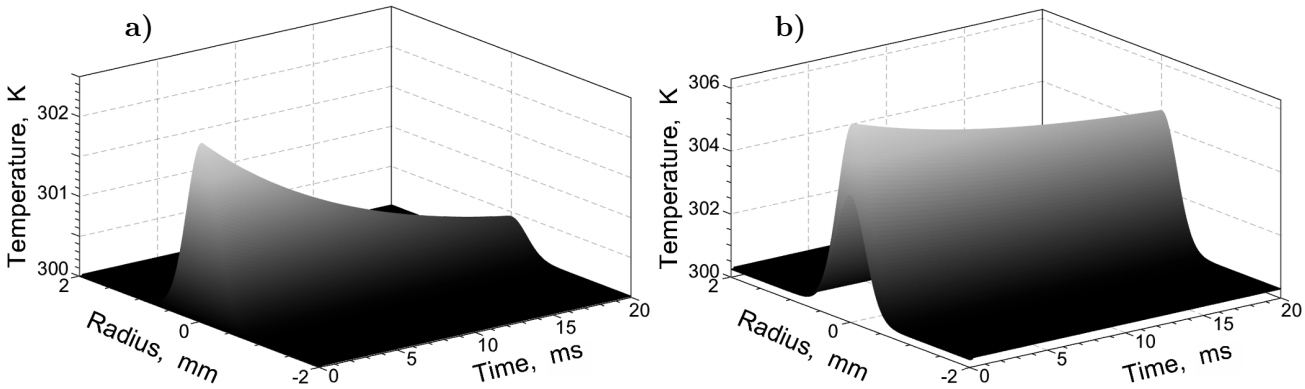


**Fig. 4.** Variation of the temperature distribution with time at 50 Hz at the first pump period (a) and at the tenth pump period (b).

In the first pump period, the upward trend of the crystal temperature with the pump duration is consistent with Fig. 3 a. However, at the end of the first pump period, the temperature has an envelope that decreases radially from the crystal center (300.44 K). Therefore, after iteration, a temperature envelope also appeared at the beginning of the tenth pump period; see Fig. 4 b. On the basis of the envelope, the crystal temperature increases linearly with the injection of pump light. The center temperature in the crystal at the end of the pump duration is 306.28 K. Relative to Fig. 4 a, the trend in the temperature decrease during the pump-free duration is slower. The crystal center temperature is 304.52 K at the end of the pump period. In the tenth pump period, the temperature difference between the end of the pump duration and the end of this period is 1.76 K. This is slightly smaller than the 1.79 K temperature difference in the first pump period. Therefore, the continuity and rationality of our quasi-steady-state thermal model are verified.

## 4. Analysis of the Transient Thermal Focal Length Variation

According to the analysis, in view of the quasi-steady-state thermal model, we provide the phase difference introduced by the thermal lens, when considering the propagation of the paraxial coherent beam along the $z$ direction [18]; it is

$$\Delta\psi = \frac{kr^2}{2f}, \tag{11}$$

where $k$ is the wave vector, $r$ is the effective radius of the pump light, and $f$ is the thermal focal length. The relationship between the optical path difference (OPD) and the phase difference reads

$$\Delta\psi = k \cdot \mathrm{OPD}. \tag{12}$$

Now it is not difficult to arrive at the expression for the OPD caused by the temperature gradient, namely,

$$\mathrm{OPD} = \int_0^l \frac{dn}{dT} \cdot \Delta T \, dz, \tag{13}$$

where $\dfrac{dn}{dT}$ is the refractive-index temperature coefficient of the crystal, and $\Delta T$ is the temperature-difference between the radial center of the crystal and any other position.

### 4.1. Solution of the Transient Thermal Focal Length in the First Pump Period

We can write the expression for the thermal focal length during the pump duration, in the first pump period; it reads

$$f_h(t) = \frac{\pi\omega_p^4\rho c}{8\,L\,\dfrac{dn}{dT}\cdot\alpha\eta P_{\text{in}}t}. \tag{14}$$

From time continuity, the expression of the thermal focal length during the pump-free duration in the first pump period is

$$f_d(t) = f_h(t_p)\exp\left[\left(\frac{\beta\lambda}{\rho c}\right)t\right]. \tag{15}$$

From Eqs. (14) and (15), the transient thermal focal length during the first period under 50-Hz pumping is shown in Fig. 5.

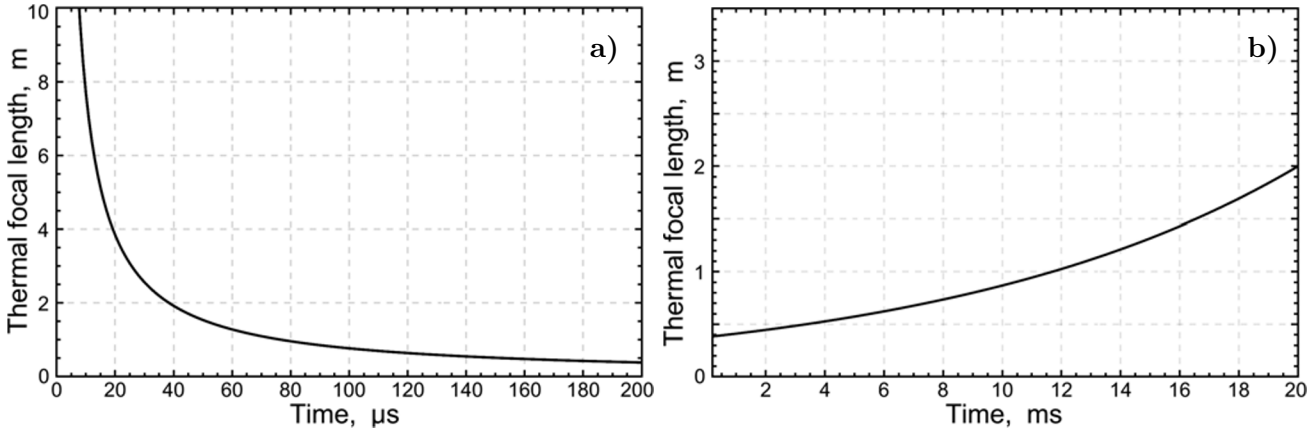


**Fig. 5.** The transient thermal focal length in the first pump period during the pump duration (a) and during the pump-free duration (b).

In Fig. 5 a, the transient thermal focal length decreases rapidly from infinity during the pump duration and reaches a constant value of 384.25 mm at the end of the pump duration. Figure 5 b starts at the end of the pump duration, and the rate of increasing thermal focal length with time in the pump-free duration is much smaller than that for the pump duration. At the end of the first period, the thermal focal length does not return to its initial state, but remains at 1996.34 mm.

### 4.2. Solution of the Transient Thermal Focal Length in Periodic Pumping

The functional expression of the transient thermal focal length in the quasi-continuous periodic pump mode is given as follows:

$$f = \begin{cases} \dfrac{\pi\omega_p^4\rho c}{\dfrac{dn}{dT}\,8\,L\alpha\eta P_{\text{in}}(t-nT+\omega_n)}, & nT \le t < nT+t_p, \\ \dfrac{\pi\omega_p^4\rho c}{\dfrac{dn}{dT}\,8\,L\alpha\eta P_{\text{in}}(t_p+\omega_n)}\exp\left[\dfrac{\beta\lambda}{\rho c}\,(t-t_p-nT)\right], & nT+t_p \le t < (n+1)T. \end{cases} \tag{16}$$

Here, $n = 0, 1, 2, \ldots$ denotes the number of periods, and $\omega_n$ is a specific parameter under different periods,

$$\omega_n = \begin{cases} 0, & n = 0, \\ \dfrac{t_p + \omega_{n-1}}{\exp\left[(T - t_p)\beta\lambda/\rho c\right]}, & n = 1, 2, 3, \ldots \end{cases} \tag{17}$$

For a 50 Hz pump repetition frequency, the transient thermal focal lengths for the first and multiple periods are shown in Fig. 6.

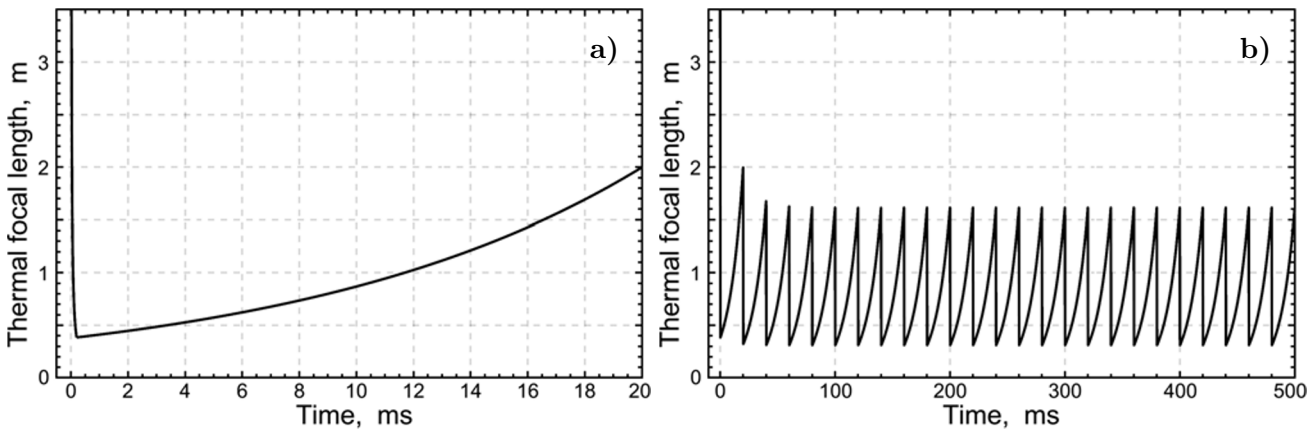


**Fig. 6.** The variation of transient thermal focal length for the first period (a) and multiple periods (b).

The value during the pump duration in the first period is inversely proportional to time; see Fig. 6 a. Because the pump duration is short, the thermal focal length curve is approximately linear. In the pump-free duration, it is exponential in time. The thermal focal length cannot be restored to the initial state within that time, but instead stopped at a larger focal length before the next period. As shown in Fig. 6 b, the variation in transient thermal focal length for each period is the same. After several periods, it varied over the fixed range of 1612.4 –310.35 mm. This can be considered as a thermal equilibrium state.

### 4.3. Simplification of Transient Thermal Focal Length under Periodic Pumping

To simplify the expression of the thermal focal length, the minimum value $F_0^{(i)}$ in the $i$th period can be used. At thermal equilibrium, Eq. (16) can be simplified to be converted as follows:

$$f = \begin{cases} \dfrac{1}{\left\{\left([1/F_0^{(i)}] - [1/F_1^{(i)}]\right)[t - nT]/t_p\right\} + 1/F_1^i}, & nT \le t < nT + t_p, \\ F_0^{(i)} \exp\left[(t - nT - t_p)\beta\lambda/\rho c\right], & nT + t_p \le t < (n+1)T. \end{cases} \tag{18}$$

where $n = 0, 1, 2, 3, \ldots$, and $F_1^{(i)}$ denotes the value at the end of the $i$th period.

In Fig. 7, we show the variation in transient thermal focal length after simplification, in view of thermal equilibrium.

If $F_0$ is the minimum thermal focal length of the first period, and $F_1$ is that at the end of the first period, then the dynamic range of the transient thermal focal length is 1996.34 – 384.25 mm; see Fig. 7 a.

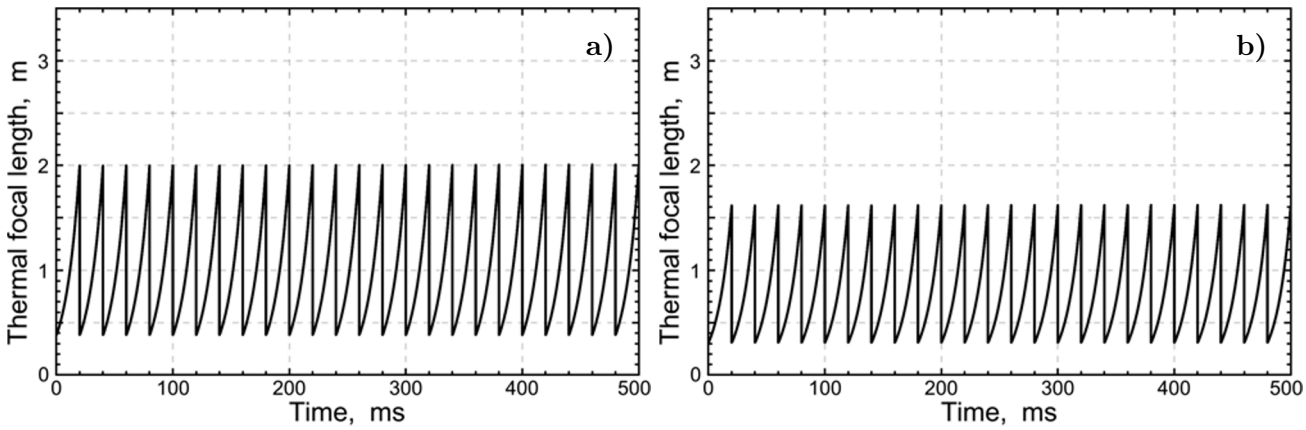


**Fig. 7.** The variation of thermal focal length under $i = 1$ (a) and $i = 4$ (a).

If $i = 4$, the dynamic range becomes 1612.8 – 310.43 mm; see Fig. 7 b. The dynamic range has a certain deviation, because only the value in the first pump period decreases from infinity. During the pump-free duration, the value cannot be restored to infinity. Therefore, at the beginning of the second period, the thermal focal length changes from a finite value, and, when Eq. (18) is used to simulate the transient thermal focal length, it is necessary to select the appropriate period $i$, according to the given pump frequency. There is a small difference between the results shown in Figs. 7 b and 6 b. This is affected by the approximately linear trend of the thermal focal length during the pump duration.

According to the quasi-steady-state thermal model, under quasi-continuous LD periodic pumping, the temperature in the crystal and the transient thermal focal length vary periodically with time. The pump period and pulse width affect the variation range of the transient thermal focal length at thermal equilibrium, and also affect the change rate during the pump-free duration. Furthermore, the crystal length and radius, as well as the pump power and beam radius, affect the transient thermal focal length. Therefore, according to our quasi-steady-state thermal model, under quasi-continuous LD periodic pumping, the adverse effects of the transient thermal focal length in a LD-pumped Nd : YAG laser design can be avoided with different pump source parameters.

### 4.4. Further Analysis of the Thermal Focal Length under High Power Pumping

Under high-power pumping, it is also necessary to consider thermal lens aberration caused by an uneven refractive index distribution. As described in [20], at higher pump densities, thermal deformation of the crystal surface caused nonparaxial wave front distortion, resulting in multimode generation. In this case, the transient thermal lens in the crystal could not be approximated by an ideal lens. In the micro-element method, the thermal lens is equivalent to a superposition of an infinite number of small lenses, and an equivalent transient thermal focal length is obtained. Nonparaxial wave front distortion will be a future research focus in a study regarding the effects of pump-source characteristic parameters on the variation range and trends of transient thermal focal lengths.

## 5. Summary

In this paper, we developed a quasi-steady-state thermal model under quasi-continuous LD periodic pumping. A quasi-adiabatic model during the pump duration and the quasi-steady-state heat dissipation model during the pump-free duration were formulated. The dynamic temperature distribution changed in the crystal and the dynamic changes in the thermal focal length caused by the thermal distributions were analyzed. In the quasi-steady-state thermal model, the temperature in the crystal increased linearly with time and the transient thermal focal length decreased inversely with time during the pump duration in each period. During the pump-free duration in each period, the temperature in the crystal decreased exponentially with time, while the transient thermal focal length increased exponentially with time.

According to the specific heat dissipation boundary conditions in the quasi-steady-state heat dissipation model, the heat in the crystal formed a stable temperature-difference distribution under a heat source with known average power. Therefore, for a known heat source distribution, the developed temperature-difference distribution function could be used to quickly construct a steady-state heat dissipation system under any power. This method could be applied to other laser crystals with thermal problems, and provides a theoretical guidance for laser design. The effect of pump-source characteristic parameters on the variation range and trend of the transient thermal focal length will be the next focus of our study.

## Acknowledgments

We thank Liwen Bianji (Edanz) (www.liwenbianji.cn) for editing the language of this manuscript.

## References

1. Di Lin and W. A. Clarkson, *Opt. Lett.*, **42**, 2910 (2017).
2. K. Schuhmann, K. Kirch, F. Nez, et al., *Appl. Opt.*, **55**, 9022 (2016).
3. E. Xing, J. Rong, S. Ying, et al., *Appl. Phys. Express*, **11**, 62702 (2018).
4. Q. Yin, H. Lu, and K. Peng, *Opt. Express*, **23**, 4981 (2015).
5. R. Bhandari and T. Taira, *Opt. Express*, **19**, 19135 (2011).
6. B. Chen, Y. Chen, J. Simmons, et al., *Appl. Phys. B*, **82**, 413 (2006).
7. S. Toroghi, A. K. Jafari, and A. H. Golpayegani, *Opt. Laser Technol.*, **41**, 800 (2009).
8. X. L. Song, G. Zhen, B. B. Li, et al., *Acta Phys. Sin.-Ch. Ed.*, **58**, 3 (2009); DOI: 10.3321/j.issn:1000-3290.2009.03.051
9. S. Wang, H. J. Eichler, X. Wang, et al., *Appl. Phys.*, **95**, 721 (2009).
10. B. Yao, T. Yi, W. Wei, et al., *Chin. Opt. Lett.*, **8**, 996 (2010).
11. B. Q. Yao, P. B. Meng, G. Li, et al., *J. Opt. Soc. Am. B*, **28**, 1866 (2011).
12. X. Lu, J. Wang, Y. Jiang, et al., *J. Mod. Opt.*, **59**, 354 (2012).
13. V. Sazegari, M. Reza Jafari Milani, and A. Khayat Jafari, *Appl. Opt.*, **49**, 6910 (2010).
14. P. Shang, M. Wu, S. Wang, et al., *Opt. Commun.*, **507**, 127676 (2022).
15. L. Li, W. Dong, J.-P. Nie, et al., *Laser Technol.*, **35**, 94 (2011) [in Chinese].
16. D. R. Poirier and G. H. Geiger, "Conduction of heat in solids," in: *Transport Phenomena in Materials Processing*, Springer, Cham (2016).
17. N. Hodgson and A. Caprara, *Appl. Opt.*, **55**, 10146 (2016).
18. Y. Xu and Y. Li, *Opt. Laser Technol.*, **44**, 114 (2012).
19. Y. Peng, Z. Cheng, Y. Zhang, et al., *Appl. Opt.*, **40**, 4824 (2001).
20. J. K. Jabczynski and K. Kopczynski, *Proc. SPIE*, **2778**, 666 (1996).